

Modelling of Cascade Fin Aerodynamics Near Stall using Kirchhoff's Steady-state Stall Model

Rakesh Kumar, Ajay Misra, and A.K. Ghosh

Indian Institute of Technology, Kanpur

E-mail: rakpec@iitk.ac.in, majay@iitk.ac.in, akg@iitk.ac.in

ABSTRACT

Nonlinear longitudinal aerodynamics associated with cascade fins at high angles of attack near stall has been modelled using Kirchhoff's formulation. Grid fins are a relatively recent development in guided missile technology. In this paper, a new category of grid fins, nomenclatured as cascade fins, has been proposed. In cascade fin design, an appropriate selection of gap-to-chord ratio and the number of planar members lead to desired stall angle and acceptable overall lift coefficient, respectively. Kirchhoff's steady-state stall model has been validated on wind tunnel data generated for Cascade fins having rectangular airfoil cross-section. National Wind Tunnel Facility (NWTF) of IIT, Kanpur, was used to generate the wind tunnel data consisting of the variation of lift coefficient with angle of attack. The cascade fins were tested to generate the data by varying gap-to-chord ratio and number of planar fins. The cascade fins with rectangular cross-section were tested with and without end plates. Kirchhoff's steady-state stall model was applied to wind tunnel data of cascade fins for modelling flow separation point and maximum likelihood method was used to estimate the parameters characterising stall characteristics. The effects of end plates, variation of number of fins and gap-to-chord ratio on parameter estimation were also studied. It has been observed that Kirchhoff's steady-state stall model could advantageously be applied to model nonlinear aerodynamics associated with cascade fins at high angle of attack.

Keywords: Cascade fin, aerodynamics, Kirchhoff's steady-state stall model

NOMENCLATURE

a_1	Static stall characteristics parameter
A	Aspect ratio
C_L	Lift coefficient
C_{L0}	Lift coefficient at zero angle of attack
$C_{L\alpha}$	Lift curve slope, $(\partial C_L / \partial \alpha)$
S_{ref}	Reference area
$S_{exposed}$	Exposed area
X	Describes the instantaneous location of an idealised flow separation point along the chord on the upper surface of the wing
X_0	Steady-state flow separation point
α	Angle of attack
α^*	Break point corresponding to $X_0=0.5$
Λ	Sweep angle

Abbreviations

<i>AF, FP</i>	Airfoil and flat plate
<i>EPY, EPN</i>	With and without end plate

1. INTRODUCTION

Grid fins, sometimes also called lattice fins, are a relatively recent development in guided missile technology¹. Unlike conventional planar fins, grid fins do not experience classical stall at high angles of attack. This leads to more

effective stability and control characteristics at intermediate and large angles of attack²⁻⁵. The main drawback of lattice fin is high drag and low aerodynamic efficiency.

To increase aerodynamic efficiency, several routine approaches to reduce drag of such lattice fins are being followed. However, in this study, a new category of grid fins, nomenclatured as Cascade fins has been proposed. A cascade fin has planar members placed parallel to each other at a distance based on an optimised gap-to-chord ratio. It is the absence of cross member that makes a cascade fin different from grid fins. In cascade fin design, the appropriate selection of gap-to-chord ratio and the number of planar members in cascade lead to desired stall angle and acceptable overall lift coefficient, respectively.

Unsteady aerodynamics has been a subject of extensive investigations. Under stationary attached flow conditions, aerodynamic effects can be adequately described using time-invariant parameters and linear models. But at higher angles of attack, models are highly nonlinear due to dominant unsteady effects and flow separation⁶. The models based on computational fluid dynamic methods, wind tunnel tests and semi-empirical formulations⁶ provide a basis for analytical investigations of the complex flow phenomena, but postulating them in an analytical form suitable for parameter estimation is difficult. Burkhalter⁷⁻⁹, *et al.* proposed aerodynamic model

to represent longitudinal aerodynamics of lattice/grid fins. The postulated model has been found quite associate up to an angle of attack of around 20°. The model⁷⁻⁹ fails to capture nonlinear aerodynamics of such fins at extended angles of attack (20-50°).

The present study is aimed for arriving at a suitable model that could be used for parameter estimation from flight data of vehicles having lattice/cascade fins. The form of proposed⁷⁻⁹ aerodynamic model has not been found amenable for parameter estimation. An alternative approach¹⁰⁻¹¹ to describe analytically the flow separation as a function of an internal state variable has been followed in the present study. Since the approach retains the state-space formulation, it is also directly amenable to identification and validation from the flight data¹²⁻¹⁴.

In the present study, Kirchhoff's model^{6,15} has been applied to aerodynamic data generated through wind tunnel testing to capture the nonlinear cascade fin aerodynamics. The experiments were conducted in wind tunnel to generate variation of lift coefficient (C_L) with angle of attack (α) up to an angle of attack of 53°. These sets of data were used to validate Kirchhoff's steady-state stall models. The effect of end plates, variation of number of fins, and gap-to-chord ratio on estimation have also been studied. The results have been presented in graphical and tabular forms and have been compared with the reference results¹⁵. It was observed that Kirchhoff's steady-state model was found suitable to model the nonlinear cascade fin aerodynamics near stall region.

2. MODEL GEOMETRIES AND EXPERIMENTAL SET-UP

2.1 Model Geometries

Cascade fin models with rectangular and airfoil cross-section were fabricated and tested in NWTF. All the planar fin models were having length, chord, planar area and aspect ratio of 0.2 m, 0.1 m, 0.02 m² and 2, respectively. Reynolds number of 253,000 based on fin-chord was used.

All the cascade fins models were categorised in two series such as FP series and AF series. The terminology 'FP series' has been used for cascade fin models with rectangular cross-section while the cascade fin models with airfoil cross-section have been termed as 'AF series'. FP series consisted of cascade fins with and without end plates having different gap-to-chord ratios and number of fins. However, AF series models were tested without end plates for different gap-to-chord ratios but for fixed number of fins.

Alpha-numeric terminology was used to completely define the various cascade fin models. For example, in the terminology xxxx_x.xx (FPC4_0.5Y or AFC4_0.5N), first two characters define the series (FP or AF), third and fourth character define number of planar fins in the cascade, next three characters after underscore () represent the gap-to-chord ratio and last character defines the status whether the cascade is with or without end plate (Y and N for with and without, respectively).

Table 1. Cascade fin models

AF series [EPN]			FP series [EPN and EPY]		
Nomenclature	No. of fins	g/c ratio	Nomenclature (X=N and Y)	No. of fins	g/c ratio
			FPC3_0.5X	3	0.5
AFPC4_0.5N	4	0.5	FPC4_0.5X	4	0.5
AFPC4_0.6N	4	0.6	FPC4_0.6X	4	0.6
AFPC4_0.7N	4	0.7	FPC4_0.7X	4	0.7
AFPC4_0.8N	4	0.8	FPC4_0.8X	4	0.8
AFPC4_0.9N	4	0.9	FPC4_0.9X	4	0.9
			FPC5_0.5X	5	0.5

Tables 1 present the terminology used to represent model configurations of FP and AF series. Model configuration fabricated and tested with and without end plates for FP series and AF series without end plates are presented in Table 1.

Figure 1(a) presents the model geometry of FP series without end plate whereas Fig. 1(b) shows the model geometry of FP series with end plate both having three fins and gap-to-chord (g/c) ratio of 0.5. Figure 2 presents the model

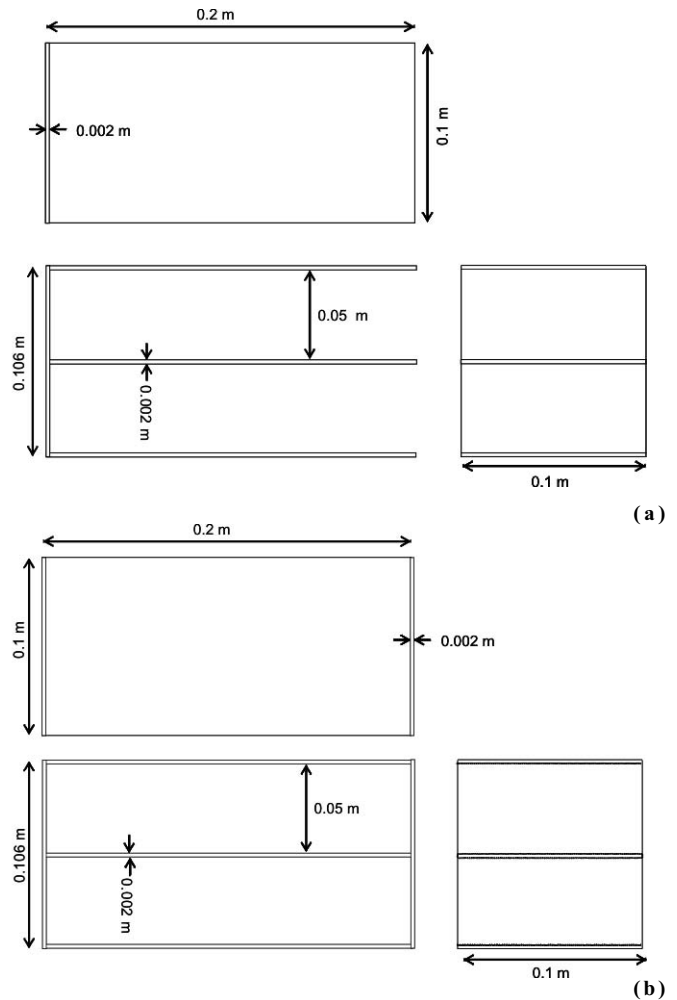


Figure 1. (a) Schematic of cascade fin model; FPC3_0.5N, (b) schematic of cascade fin model; FPC3_0.5Y.

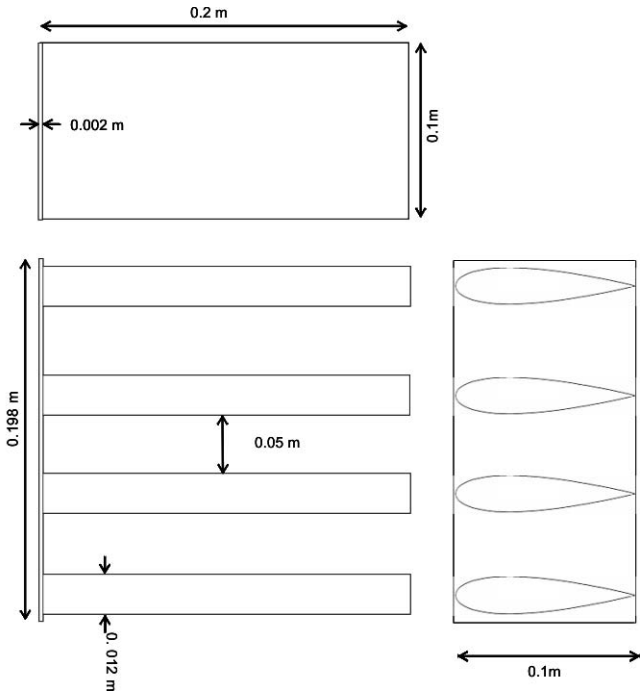


Figure 2. Schematic of cascade fin model; AFC4_0.5N.

geometry of AF series without end plate having four planar fins and *g/c* ratio of 0.5.

Figures 1 and 2 also show the other geometrical parameters such as length (0.2 m), chord (0.1 m), aspect ratio (2), thickness of the planar fins of FP series (0.002 m) and AF series (0.012m) and gap (0.05 m) between two planar fins. The thickness of base plate and end plate was 0.002 m. Other cascade planar fin models (Tables 1 and 2) were having similar geometric configurations. NACA 0012 airfoil section was used to fabricate the planar fins of AF series.

2.2 Experimental Setup

Figure 3 shows the schematic of experimental setup in wind tunnel for cascade fin models. Planar fins were mounted on the balance which was fixed vertically on a turn table of the tunnel floor through front- and rear-end adaptors. A shroud was placed over the balance, front- and rear-end adaptors to isolate balance from direct wind loads.

As no part of the mounting assembly was either upstream or downstream of the fin model, the interference caused by mounting assembly on the fins was minimal. The only interference, the fins could feel, was due to transverse disturbance caused by flow over vertical, cylindrical shroud. Such a transverse disturbance caused by a non-rotating cylindrical shroud could be because of imperfections of the cylindrical shroud, the flow angularity, and the flow around the upper tip of the vertical cylindrical shroud. The single planar fins and cascade fins were mounted on top of the vertical assembly using a base plate.

A medium load range 6-component strain gauge balance was used to measure the forces and moments on aircraft model during the experiment. The schematic and actual

load balance (BA 050_D60_L425) of type-D have been shown in Fig. 4. The load balance was 425 mm long and was having maximum diameter of 60 mm.

The load balance was having a sensitivity of 0.1 per cent. The balance was made of stainless steel (17-4-PH) with yield strength of about 118 kg/mm². The balance consisted of two normal force gauge stations, two side force gauge stations, two axial force measuring bridges, and one rolling moment bridge.

Digital data acquisition system was used to obtain the wind tunnel data. Wind tunnel tests were conducted at *V* = 40 m/s. The planar fins were tested at Reynolds number of 253,000. The density of air was taken to be 1.2 kg/m³ for the computation of dynamic pressure and Reynolds number.

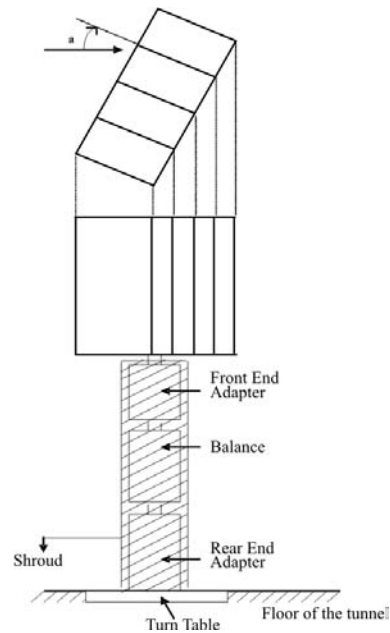


Figure 3. Experimental setup for cascade fins.

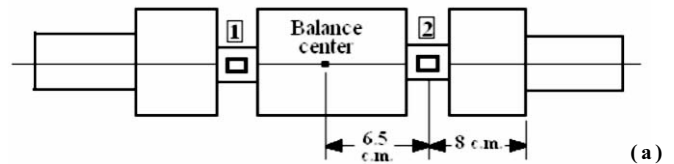


Figure 4. (a) Schematic, and (b) actual load balance of type-D.

3. GENERATION OF LONGITUDINAL AERODYNAMIC DATA

Cascade fins with rectangular (FP Series) and airfoil (AF Series) cross-sections were tested in NWTF to generate wind tunnel data at $V=40$ m/s simulating Reynolds number of 253000 using non-dimensional length of 0.2. The reference area used was 0.02 m². The tests were conducted to generate the variation of C_L with α (up to $\sim 53^\circ$).

3.1 FP Series

In case of FP series with planar fins having thickness-to-chord ratio of 0.02, the tests were conducted by varying gap-to-chord (g/c) ratio and number of fins. The leading edges of the fins were smoothed to remove sharp edges. These tests were conducted with and without end plates to see the effect on Modelling and estimation.

Figures 5 to 9 present the variation of C_L with α for g/c ratios of 0.5, 0.6, 0.7, 0.8, and 0.9, respectively without end plate having number of planar fins equal to four. It can be observed [Figs (5-9)] that variation of C_L with α up to angles of attack of around 15° is fairly linear but becomes nonlinear beyond 15° . It can also be observed that the stalling angle and maximum lift coefficient (C_{Lmax}) continuously increase with increase in g/c ratio.

Tests were also conducted for cascade fin models (FP Series) with end plate to generate the data of C_L with α for g/c ratios of 0.5, 0.6, 0.7, 0.8, and 0.9 consisting of four planar fins. In this case also, it was observed (not shown) that the variation of C_L with α up to angles of attack of around 15° was fairly linear but became nonlinear beyond 15° . Also, the stalling angle was continuously increasing with increase in g/c ratio.

Next, the tests for FP series were conducted by varying the number of fins in the cascade with and without end plates. The tests were conducted for different number of planer fins in the cascade with g/c ratio of 0.5. In this case, it was observed that the variation of C_L with α up to angles of attack of around 15° was fairly linear but became nonlinear beyond 15° . It was also observed that the C_{Lmax} was continuously increasing with increase in number of planar fins.

Similar behaviour was observed when the testing was conducted with end plates for different number of planar fins.

3.2 AF Series

Next, model geometries of AF Series (NACA 0012) were tested without end plates. The g/c ratio was varied while conducting wind tunnel tests. The number of planar fins used while conducting the tests was four. Figures 10-14 present the variation of C_L with $-\alpha$ for g/c ratios of 0.5, 0.6, 0.7, 0.8, and 0.9, respectively for cascade fin models with four fins (without end plates).

It can be observed [Figs (10-14)] that the linear portion of the variation of C_L with α was continuously decreasing with increase in g/c ratio. It was also observed that the C_{Lmax} increased with increase in g/c ratio.

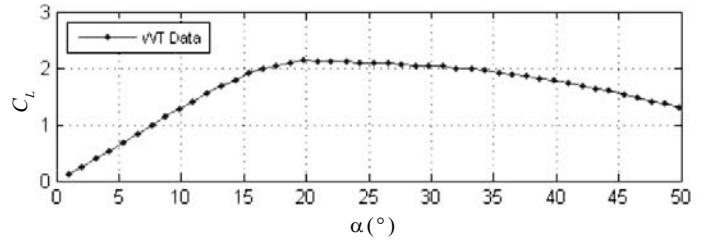


Figure 5. Variation of C_L with α ; FPC4_0.5N.

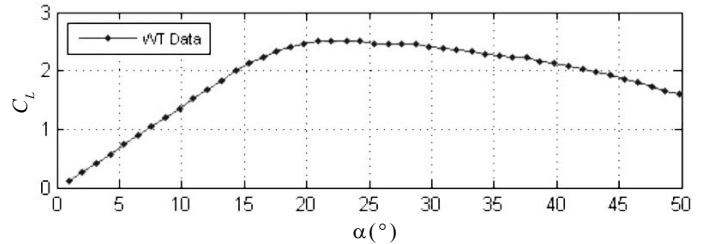


Figure 6. Variation of C_L with α ; FPC4_0.6N.

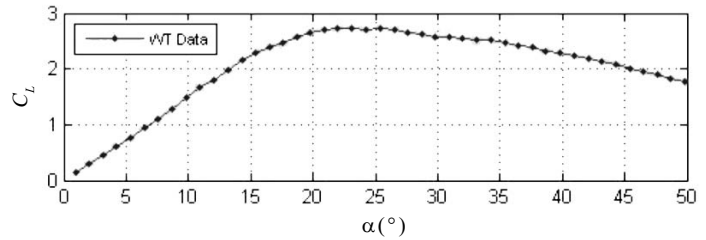


Figure 7. Variation of C_L with α ; FPC4_0.7N.

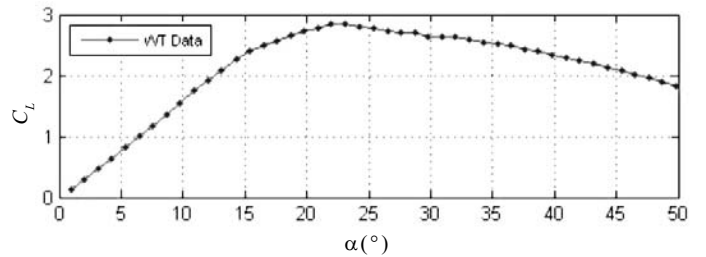


Figure 8. Variation of C_L with α ; FPC4_0.8N.

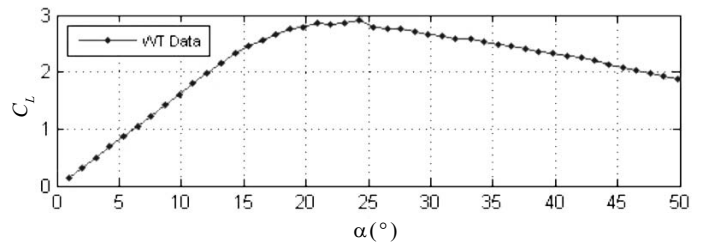
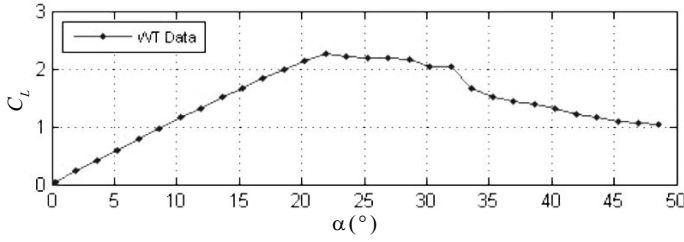
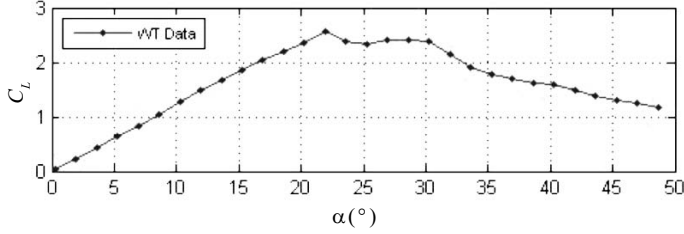
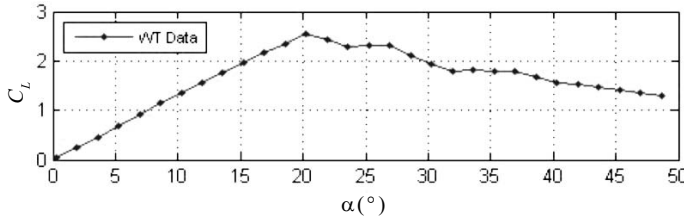
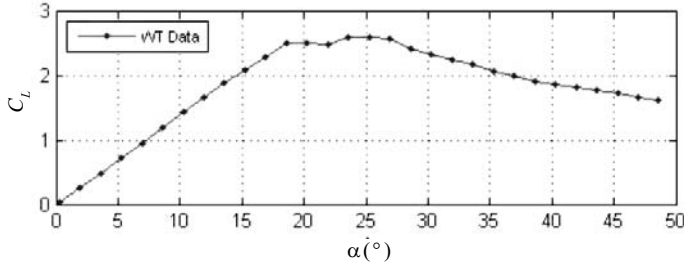
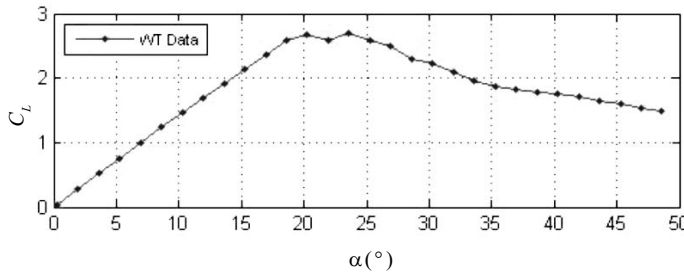


Figure 9. Variation of C_L with α ; FPC4_0.9N.

If one compares FP series [Figs (5-9)] and AF series [Figs (10-14)] wrt the variation of C_L with α , it could be observed that AF series fins experienced extended stall characteristics. A noticeable difference in the post-stall/near-stall characteristics could be observed between FP series and AF series fins. Similar trends were also observed (not shown) for pitching-moment characteristics.


 Figure 10. Variation of C_L with α ; AFC4_0.5N.

 Figure 11. Variation of C_L with α ; AFC4_0.6N.

 Figure 12. Variation of C_L with α ; AFC4_0.7N.

 Figure 13. Variation of C_L with α ; AFC4_0.8N.

 Figure 14 Variation of C_L with α ; AFC4_0.9N.

4. STEADY-STATE STALL MODELLING

Aerodynamic models become highly nonlinear due to dominant unsteady effects and flow separation at high angles of attack. For such a case, based on Kirchhoff's theory of flow separation for a symmetrical profile, the lift can be modelled as a function of angle of attack (α) and flow separation point⁶:

$$C_L(\alpha, X) = C_{L\alpha} \left\{ \frac{1 + \sqrt{X}}{2} \right\}^2 \alpha \quad (1)$$

where $C_{L\alpha}$ is lift curve slope and is given as

$$C_{L\alpha_i} = \frac{(2\pi A)}{\left(2 + \sqrt{4 + \frac{A^2 \beta^2}{\eta^2} \left(1 + \frac{\tan^2 \Lambda}{\beta^2} \right)} \right)} * \frac{S_{\text{exposed}}}{S_{\text{ref}}} \quad (2)$$

Reformulating the Kirchhoff's formulation of flow separated lift [Eqn (1)] and extending by C_{L_0} for non-symmetrical profile yields the following expression for steady-state profile of flow separation point (X_0).

$$X_0 = \left\{ 2 \sqrt{\left[(C_L - C_{L_0}) / (C_{L\alpha} \alpha) - 1 \right]} \right\}^2 \quad (3)$$

The steady-state flow separation point (X_0) depends upon the airfoil and wing configuration. Using Eqn (1) with $X = X_0$ the function can be determined statically in wind tunnel by substituting the values of $C_{L\alpha}$, C_{L_0} and C_L obtained through wind tunnel testing. It may be noted that the values of required in Eqn (3) corresponds to linear value of the lift curve slope. An alternative procedure has been used in this study wherein X_0 has been modelled as per Eqn (4).

$$X_0 = \frac{1}{2} \left\{ 1 - \tan h \left[a_1 (\alpha - \alpha^*) \right] \right\} \quad (4)$$

where a_1 defines the static stall characteristics of the airfoil and α^* is the breakpoint corresponding to $X_0 = 0.5$. This approximation is better suited to parameter estimation because it is a continuous function in its entire range and has just two unknown parameters (a_1 and α^*).

5. RESULTS AND DISCUSSION

Kirchhoff's theory of flow separation was applied to the wind tunnel data of cascade fins to model lift coefficient as a function of angle of attack and flow separation point.

First flow separation point was estimated using Eqn (3). The values of C_L at given α was read directly from the wind tunnel-generated data. The value of $C_{L\alpha}$ required to compute X_0 was computed using vortex lattice formulation¹⁵ (VLM). The computed value of X_0 thus obtained was referred to as $X_{0(wT)}$.

Next, the parameters characterising stall characteristics (a_1 and α^*) were estimated using Eqn (4). Maximum likelihood method was applied to minimise the error between the wind tunnel measured [$X_{0(wT)}$] and model-estimated [$X_{0(estimated)}$] value flow separation point for parameter estimation.

5.1 FP Series

Kirchhoff's steady-state stall model was applied to the wind tunnel data of FP series generated by varying g/c ratio and number of fins with and without end plates. Wind tunnel-measured [$X_{0(wT)}$] and model-estimated [$X_{0(estimated)}$] flow separation point as a function of α have been compared.

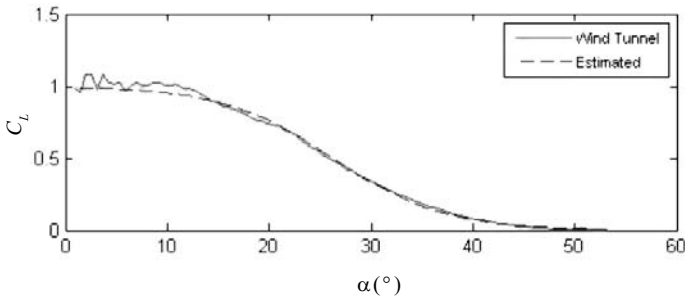


Figure 15. Measured and estimated X_0 ; FPC3_0.5Y.

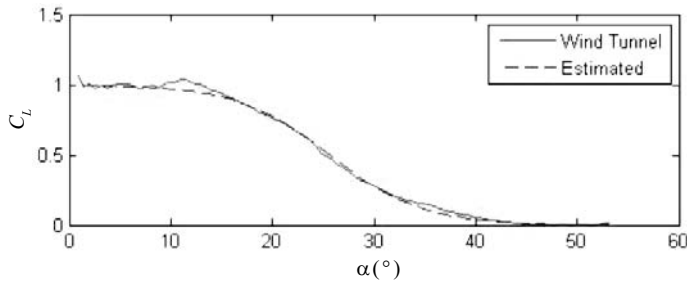


Figure 16. Measured and estimated X_0 ; FPC4_0.5Y.

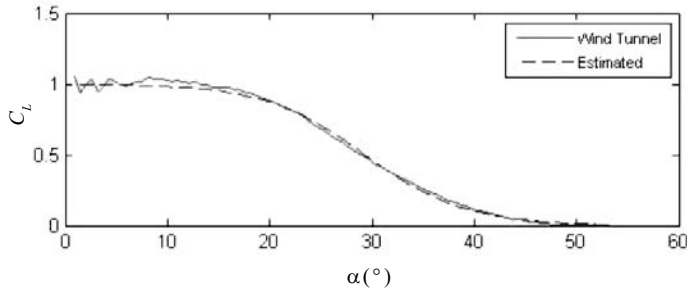


Figure 17. Measured and estimated X_0 ; FPC5_0.5Y.

Next, the comparison between $X_{0(WT)}$ and $X_{0(estimated)}$ for different number of planar fins for FP series with [Figs (15-17)] and without (not shown) end plates was made. It can also be observed from figures that the matching of flow separation point (X_0) shows the deterioration for cascade having number of planar fins equal to three and five. Similar trend was observed when the comparison was made for cascade without end plate.

First, Kirchhoff's steady-stall model using maximum likelihood method was applied to wind tunnel data of FP series to see the effect of variation of number of planar fins on estimated values of a_1 and α^* . Table 2 presents the effect of number of planar fins on estimated values of a_1 and α^* for wind tunnel data of FP series. The tests were conducted for model geometries of FP series (EPY and EPN) having three, four, and five planar fins. It was observed that the estimated value of parameter α^* (break point) was slightly higher for cascade model having five planar fins (EPY and EPN).

The effect of variation of g/c ratio on parameter estimation has been presented in Tables 3 and 4 for FP series (without and with end plates). The tested cascade was having four planar fins. The g/c ratio was varied from 0.5 to 0.9 at an

Table 2. Effect of number of fins (FP series) on parameter estimation

Fin configuration	No. of planar fins	Model estimated	
		a_1	α^* [deg]
FPC3_0.5Y	3	5.272 (0.038)	26.2 (0.0008)
FPC4_0.5Y	4	6.257 (0.049)	25.6 (0.0007)
FPC5_0.5Y	5	5.869 (0.045)	29.3 (0.0007)
FPC3_0.5N	3	4.954 (0.034)	23.9 (0.0008)
FPC4_0.5N	4	7.084 (0.059)	23.8 (0.0007)
FPC5_0.5N	5	6.187 (0.048)	28.5 (0.0007)

() Cramer-Rao bounds

Table 3. Effect of g/c ratio (FP series with EPN) on parameter estimation

Fin configuration	g/c ratio	Model estimated	
		a_1	α^* [deg]
FPC4_0.5N	0.5	7.084 (0.059)	23.8 (0.0007)
FPC4_0.6N	0.6	6.416 (0.051)	25.2 (0.0007)
FPC4_0.7N	0.7	5.277 (0.038)	23.9 (0.0008)
FPC4_0.8N	0.8	5.249 (0.038)	23.2 (0.0008)
FPC4_0.9N	0.9	4.167 (0.028)	20.4 (0.0009)

() Cramer-Rao bounds

increment of 0.1. It can be observed from Tables 3 and 4 that the value of parameter a_1 keeps on decreasing with increase in g/c ratio. Similar trend was shown by the parameter α^* except for the first value corresponding to g/c ratio of 0.5. This may be due to slightly inaccurate wind tunnel data for this particular case.

However, with end plates, the trend of decrease in parameter α^* with increase in the value of g/c ratio was observed for all the values of g/c ratio. Low estimated values of Cramer-Rao bounds suggest the reasonable accuracy level of the estimation. The comparison of the estimates (Table 4) from Kirchhoff's model estimates obtained by Misra¹⁵ validates the better suitability of the former.

5.2 AF Series

In case of AF series, Kirchhoff's steady-state stall model was applied to the wind tunnel data generated by varying g/c ratio (without end plates). Wind tunnel-measured [$X_{0(WT)}$] and model-estimated [$X_{0(estimated)}$] flow separation point as a function of α (not shown) illustrated the similar trend as in case of FP series.

Table 5 presents the effect of variation of g/c ratio on parameter estimation for AF series without end plates.

It can be observed that the values of parameters a_1 and α^* do not follow the same trend as they followed in the case of FP series. The erratic behaviour in the trend may be due to noisy data gathered during the wind tunnel testing. It can be observed that similar results of estimates were obtained by Misra¹⁵ also.

6. CONCLUSION

Kirchhoff's steady stall model has been applied to wind tunnel data of cascade fin model geometries having

Table 4. Effect of g/c ratio (FP series with EPY) on parameter estimation

Fin configuration	g/c ratio	Model estimated		Ref.(15) estimated	
		α_1	α^* [deg]	α_1	α^* [deg]
FPC4_0.5Y	0.5	6.25 (0.049)	25.6 (0.0007)	5.43	25.4
FPC4_0.6Y	0.6	6.09 (0.047)	25.4 (0.0007)	5.51	26.0
FPC4_0.7Y	0.7	5.30 (0.038)	24.5 (0.0008)	5.51	25.7
FPC4_0.8Y	0.8	5.11 (0.036)	23.3 (0.0008)	5.55	25.0
FPC4_0.9Y	0.9	6.78 (0.055)	22.9 (0.0007)	6.16	23.7

Values in (): Cramer-Rao bounds

Table 5. Effect of g/c ratio (AF series with EPN) on parameter estimation

Fin configuration	g/c ratio	Model estimated		Ref.(15) estimated	
		α_1	α^* [deg]	α_1	α^* [deg]
AFC4_0.5N	0.5	9.15 (0.480)	27.7 (0.003)	10.18	29
AFC4_0.6N	0.6	8.46 (0.427)	27.5 (0.003)	8.8	27.75
AFC4_0.7N	0.7	10.20 (0.565)	25.4 (0.003)	7.62	25.75
AFC4_0.8N	0.8	8.05 (0.396)	26.3 (0.003)	7.04	26.5
AFC4_0.9N	0.9	9.72 (0.526)	25.6 (0.003)	8.12	25.5

Values in (): Cramer-Rao bounds

rectangular and airfoil cross-sections for modelling nonlinear aerodynamics near stall. The parameters characterising static stall characteristics (α_1 and α^*) were estimated using maximum likelihood method. The estimation results have also been compared with the reference results and were found even better in some cases.

In cascade fin design, the appropriate selection of gap-to-chord ratio and the number of planar members may lead to desired stall angle and acceptable overall lift coefficient, respectively. Therefore, Kirchhoff's steady-state stall model can be used suitably to capture the nonlinear cascade fin aerodynamics near stall region.

The main drawback of grid fins, also called lattice fins, is high drag and low aerodynamic efficiency. In this study, cascade fin models have been used to study the nonlinear aerodynamics using Kirchhoff's steady-state stall model. It is the absence of cross member that makes a cascade fin different from grid fins. During the study, it has been established that the desirable stall and lifting characteristics can be obtained if appropriate selection of gap-to-chord ratio and the number of planar members in cascade is made. Kirchhoff's steady-state stall model has been applied because the data pertains to wind tunnel. The presented work can be taken as baseline for the design of cascade fin-tail in guided missiles wrt desirable stall and lifting characteristics.

The work has been presented for steady-state case using Kirchhoff's steady-state stall model, however, Kirchhoff's quasi-steady-state stall model can be applied to model nonlinear aerodynamics of simulated flight data of missiles having cascade type fins.

REFERENCES

1. Fleeman, E.L. Tactical missile design. AIAA Education Series, 2001.
2. Simpson, G.M. & Sadler, A.J. Lattice controls: A Comparison with conventional planar fins. NATO Research and Technology Organisation, 1998. pp. 9.1-9.10.
3. Washington, W.D. & Miller, M.S. Grid fins- A new concept for missile stability and control. AIAA Paper 93-0035, Reston, VA, 1993. 141p.
4. DeSpirito, J.; Edge, L.H.; Weinacht, P.; Sahu, J. & Dinavahi, S. Computational fluid dynamics analysis of missile with grid fins. *J. Spacecraft Rockets*, 2001, **38**(5), 711-18.
5. Washington, W.D. & Miller, M.S. Experimental investigation of grid fin aerodynamics: A synopsis of nine wind tunnel and three flight tests. *In Symposium on Missile Aerodynamics*, Sorrento, Italy, 11-14 May, 1998. pp. 10.1-10.13.
6. Jategaonkar, R.V. Flight vehicle system identification: A time domain methodology. *AIAA Progress in Aeronautics and Astronautics*, 2006, **21**(6), AIAA, Reston, VA.
7. Burkhalter, J.E.; Hartfield, J.R. & Leleux, T.M. Nonlinear aerodynamic analysis of grid fin configurations. *Journal of Aircraft*, 1995, **32**(3), 547-54.
8. Burkhalter, J.E. & Frank, H.M. Grid fin aerodynamics for missile applications in subsonic flow. *Journal of Aircraft*, 1996, **33**(1), 5-18.
9. Burkhalter, J.E. Grid fins for missile applications in supersonics flow. *In 34th AIAA Aerospace Science Meeting and exhibition*. AIAA Paper 1996-194, 1996.
10. Leishman, J.G. & Nguyen, K.Q. State-space representation of unsteady airfoil behaviour. *AIAA Journal*, 1990, **28**(5), 836-44.
11. Goman, M. & Khrabrov, A. State-space representation of aerodynamic characteristics of an aircraft at high angles of attack. *Journal of Aircraft*, 1990, **31**(5), 1109-115.
12. Fischenberg, D. Identification of an unsteady aerodynamic

stall model from flight test data. AIAA Paper 1995-3438, 1995.

13. Greenwell, D.I. A review of unsteady aerodynamic modelling for flight dynamics of maneuverable aircraft. AIAA Paper 2004-5276, 2004.
14. Fischenberg, D. & Jategaonkar, R.V. Identification of aircraft stall behaviour from flight test data. RTO-MP-11, Paper No. 17, March 1999.
15. Misra, A. Investigation of grid and cascade fins for missile flight stabilisation and control. IIT, Kanpur, April 2009. (PhD Thesis)

papers in national/international conferences/journal. His research areas include: Flight mechanics, aerodynamics, neural networks.



Dr Ajay Misra obtained PhD (Aerospace Engineering) from IIT, Kanpur. Presently working as a Sr Research Engineer at Flight Laboratory, Department of Aerospace Engineering, IIT Kanpur. He has published more than 20 research papers in national/international conferences/journals. His research areas include Aerodynamics, flight mechanics.

Contributors



Mr Rakesh Kumar has obtained MTech (Aerospace Engineering) from Indian Institute of Technology (IIT), Kanpur in 1996. He is pursuing his PhD (Aerospace Engineering) from IIT Kanpur. Presently working as an Assistant Professor, Aerospace Engineering Department, PEC University of Technology, Chandigarh. He has published more than 20 research



Dr A.K. Ghosh obtained PhD (Aerospace Engineering) from IIT, Kanpur. Presently working as a Professor in the Department of Aerospace Engineering, IIT, Kanpur. He has published more than 50 research papers in national/international journals/conferences. He is the recipient of *DRDO Technology Award-1993*. His research areas include Flight mechanics, parameter estimation from flight data, neural modelling, design of air borne stores, aircraft bombs, artillery shells and rockets, design of control law of guided missiles.